Koninklijk Meteorologisch Instituut

Institut Royal Météorologique

Köninglische Meteorologische Institut

Royal Meteorological Institute

KMI - IRM

Testing for Dynamical Dependence: Application to the Surface Mass Balance Over Antarctica

Quentin Dalaiden°, Stéphane Vannitsem*, Hugues Goosse°

Royal Meteorological Institute of Belgium, Brussels, Belgium

°Earth and Life Institute, UCLouvain, Belgium

In a nutshell: Key messages

- The analysis of the rate of information transfer allows for clarifying dynamical dependence beyond the classical correlation analysis
- The surface mass balance over the Plateau, the central part of Antarctica, is mainly influenced by temperature and sea ice concentration
- The surface mass balance on the Weddell sea and Dronning Maud Land coasts displays a dynamics with a large influence of global-scale modes

Vannitsem, S., Dalaiden, Q., & Goosse, H. (2019). Testing for dynamical dependence: Application to the surface mass balance over Antarctica. *Geophysical Research letters*, *46*, https://doi.org/10.1029/2019GL084329

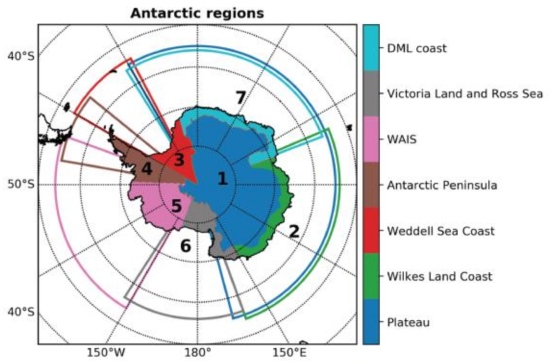

Figure 3. Regional boundaries separating the different regions used in this study. DML = Dronning Maud Land; WAIS = West Antarctica Ice Sheet.

Introduction

The Surface Mass Balance over Antarctica displays an evolution

- Highly dependent on the location (Medley and Thomas, 2019)
- With an influence of atmospheric dynamical modes (Marshall et al., 2017)
- With complex interactions with sea ice (Wang et al., 2020)

How to look in a systematic way to dependences of SMB to other observables?

Test of a technique recently introduced in the literature (Liang, 2014)

Data and Regions

MPI-ESM-P, 850-2005
CESM1, 850-2005

Era-Interim, 1979-2010
(not shown as it is inconclusive
due to the limited size of the dataset)

Atmospheric indices:

SAM
ENSO
ZW3

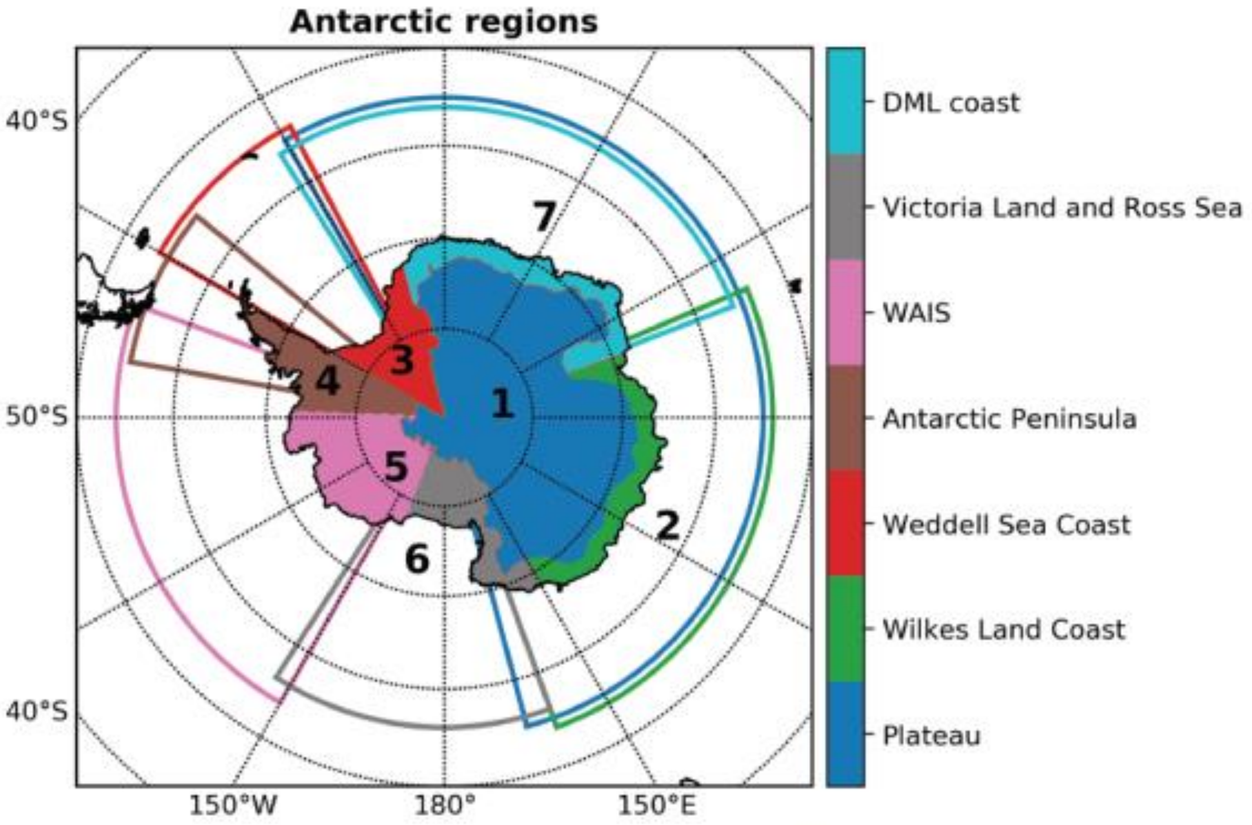

Figure 3. Regional boundaries separating the different regions used in this study. DML = Dronning Maud Land; WAIS = West Antarctica Ice Sheet.

Transfer of information, beyond correlation

(Liang and Kleeman, 2005, 2007; Liang, 2014)

Stochastic differential equations (F could be nonlinear)

$$d\mathbf{X} = \mathbf{F}(\mathbf{X};\boldsymbol{\theta})dt + \mathbf{B}(\mathbf{X};\boldsymbol{\theta})d\mathbf{W}$$

N-dimensional system

$$T_{2\to 1} = -\int_{\mathbb{R}^n} \rho_{2|1} \frac{\partial (F_1 \rho_{\not{2}})}{\partial x_1} dx + \frac{1}{2} \int_{\mathbb{R}^n} \rho_{2|1} \frac{\partial^2 (g_{11} \rho_{\not{2}})}{\partial x_1^2} dx$$

Transfer of information from variable 2 to variable 1 (with n=2):

$$T_{2\to 1} = -E\left[\frac{1}{\rho_1}\frac{\partial (F_1\rho_1)}{\partial x_1}\right] + \frac{1}{2}E\left[\frac{1}{\rho_1}\frac{\partial^2 \left(b_{11}^2 + b_{12}^2\right)\rho_1}{\partial x_1^2}\right]$$

ρ_1: probability density of variable 1
F_1: tendency for variable 1
$b_{11}$and b_{12}: noise entries of B associated with both variables

A linear system : A coupled O-U process

$$\frac{\mathrm{d}X_1}{\mathrm{d}t} = a_{1,1}X_1 + a_{1,2}X_2 + \xi_1(t)$$

$$\frac{\mathrm{d}X_2}{\mathrm{d}t} = a_{2,2}X_2 + a_{2,1}X_1 + \xi_2(t),$$

One gets

$$T_{2\to 1} = \frac{C_{11}C_{12}C_{2,d1} - C_{12}^2 C_{1,d1}}{C_{11}^2 C_{22} - C_{11}C_{12}^2}$$

where C_{11} and C_{11} are the variances, C_{12} is the covariance, and the $C_{1,d1}$ the covariance Between the variable 1 and its tendency. See Liang 2014.

This can be easily used for time series analysis

A simple example: Coupled O-U processes

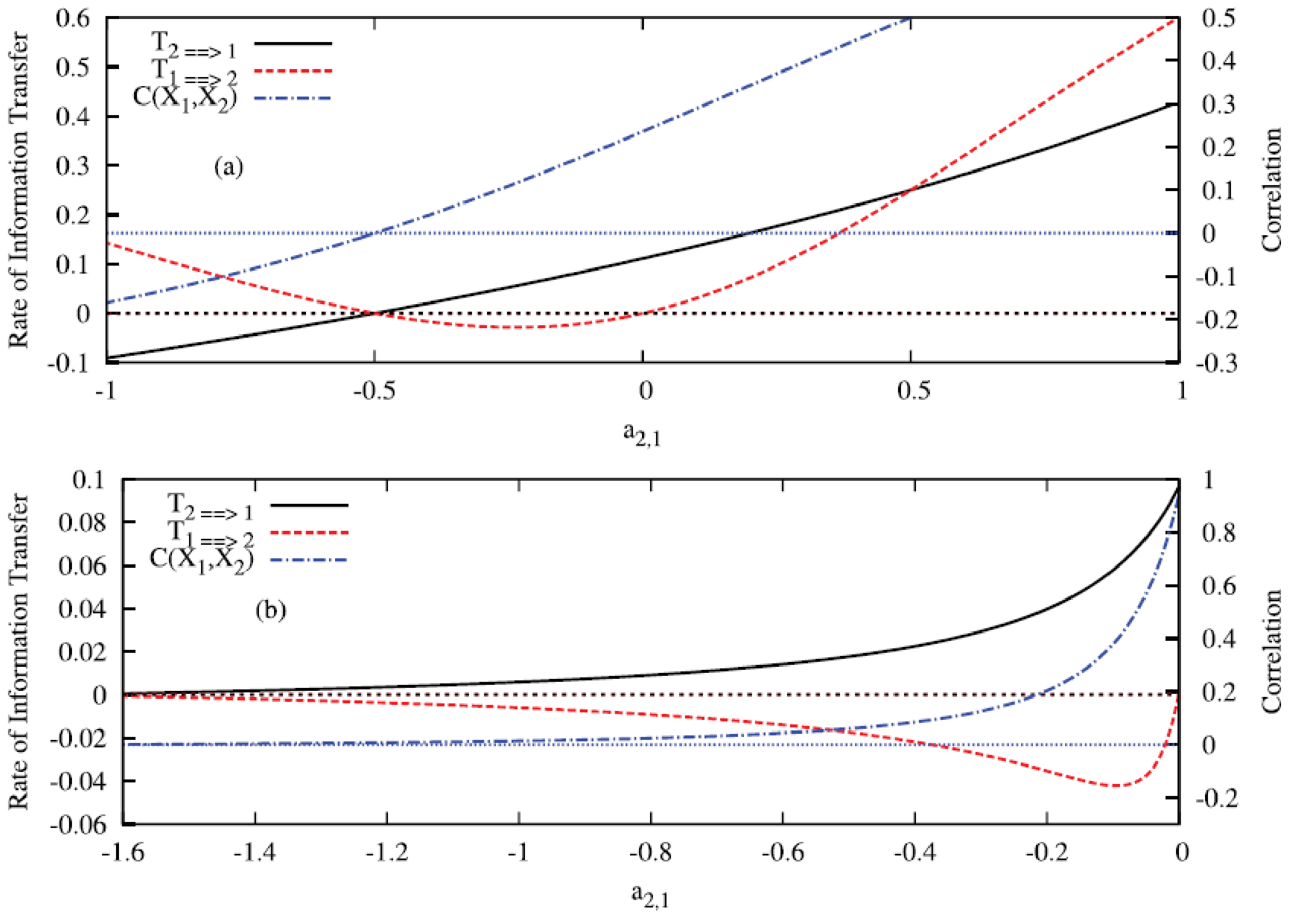

Figure 1. Theoretical values of the rate of information transfer and correlation as a function of the coefficient $a_{2,1}$ of the stochastic linear model described by equation (2). In (a), the other model parameters are fixed to $a_{1,1} = a_{2,2} = -1$ and $a_{1,2} = 0.5$ and, in (b), to $a_{1,1} = -0.1$, $a_{2,2} = -0.01$, $a_{1,2} = 0.17$. The rates of information transfer from 2 to 1 and from 1 to 2 are denoted as "$T_{2\to 1}$" and "$T_{1\to 2}$" in the legends of each panel. $C(X_1, X_2)$ denotes the correlation between X_1 and X_2.

Important features going beyond Correlation:

- Directional information on dependences

- Applicable for the comparison of time series

- No embedding necessary, as in the Convergent Cross Mapping method

Results: MPI-ESM-P

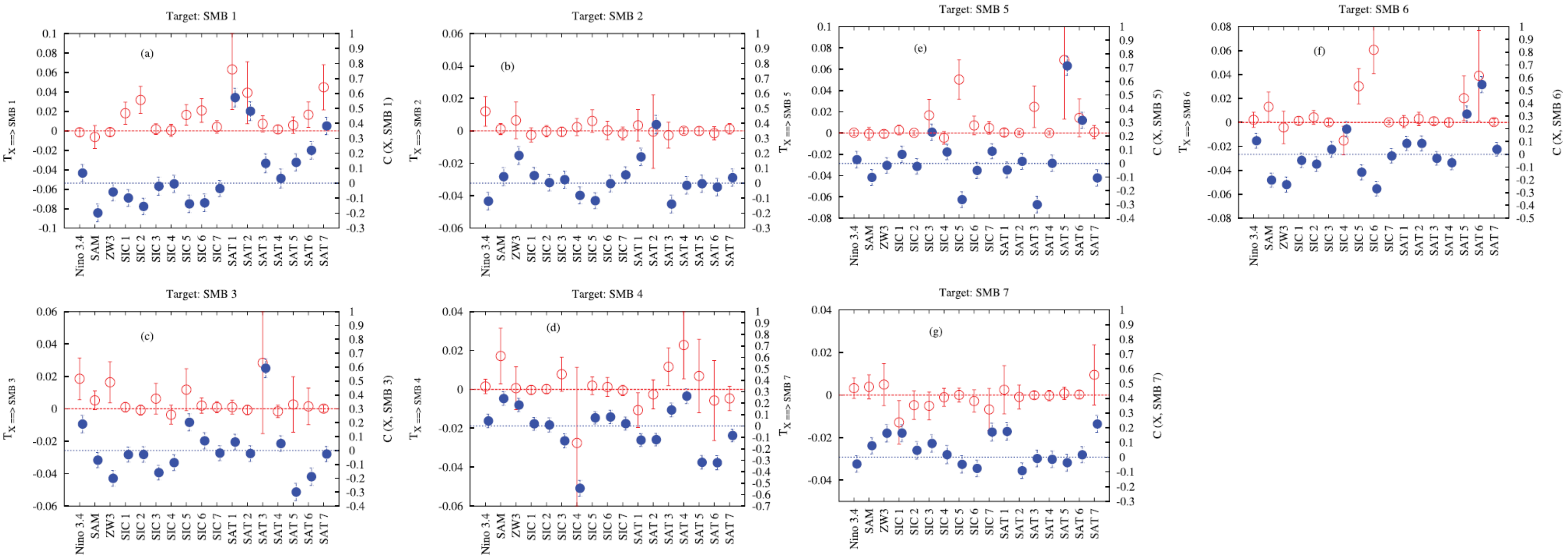

Transfer of information in red and correlation in blue. Target on top of each panel

Results: MPI-ESM-P

Dependence of SMB on Atmospheric Indices:

El-Nino influences Regions 2 and 3

SAM influences Regions 4 and 6

ZW3 influences Region 3 only

Interestingly, several highly significant correlations of ZW3 with the SMB over Regions 2, 4, 6, and 7 do not lead to any dynamical dependence

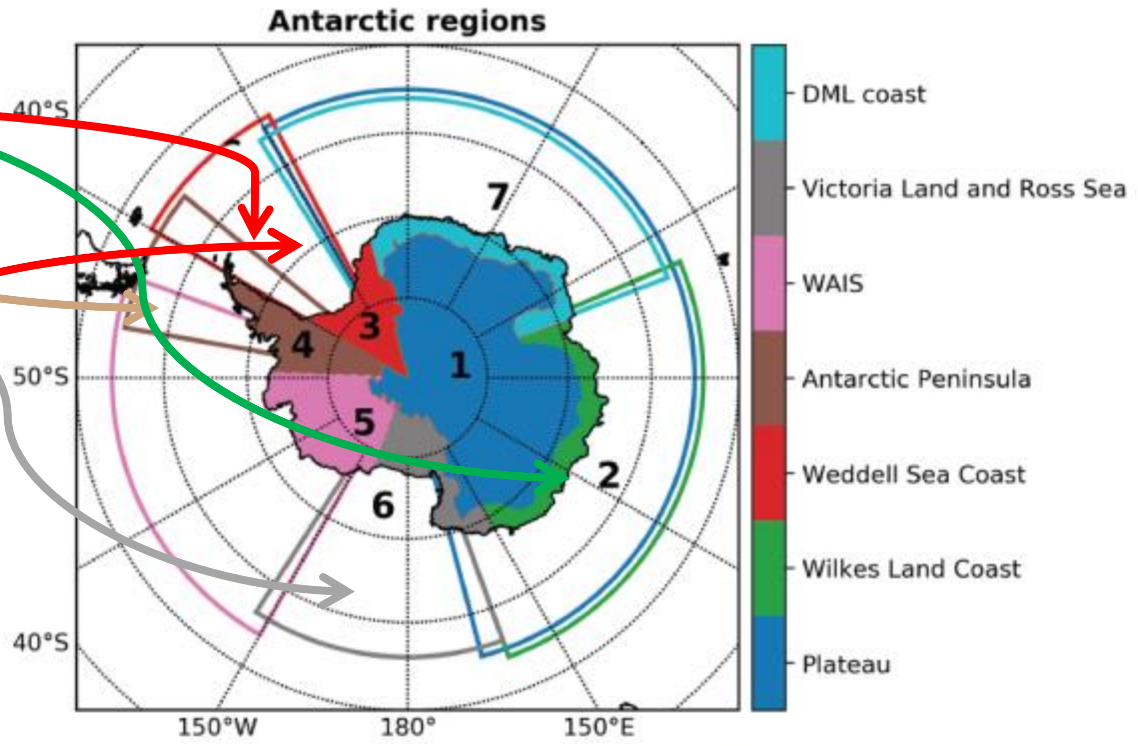

Figure 3. Regional boundaries separating the different regions used in this study. DML = Dronning Maud Land; WAIS = West Antarctica Ice Sheet.

Results: MPI-ESM-P

Dependence of SMB on Surface temperature:

Region 1: influenced by 1, 2, 6 and 7

Region 4: influenced by 3 and 4

Region 5: influenced by 3 and 5

Region 6: influenced by 5 and 6

Dependence of SMB on Sear Ice:

Region 1: influenced by 1, 2, 5 and 6

Region 5: influenced by 5

Region 6: influenced by 4, 5 and 6

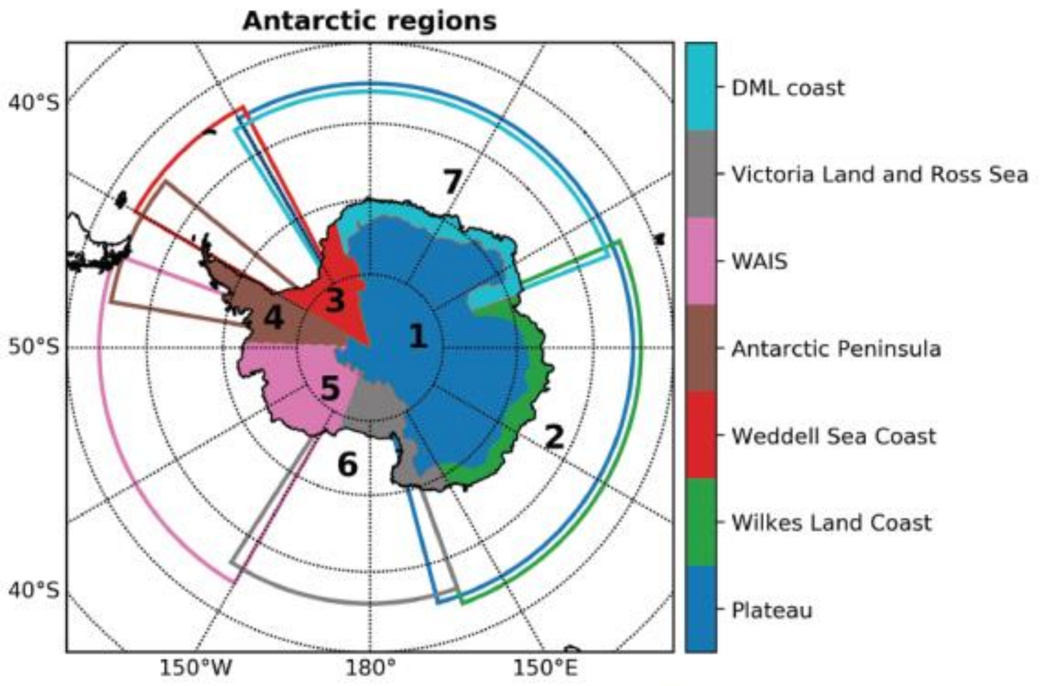

Figure 3. Regional boundaries separating the different regions used in this study. DML = Dronning Maud Land; WAIS = West Antarctica Ice Sheet.

SMB in Region 6 is not influenced by Sea Ice despite of significant correlations.

Results: CESM1-CAM5

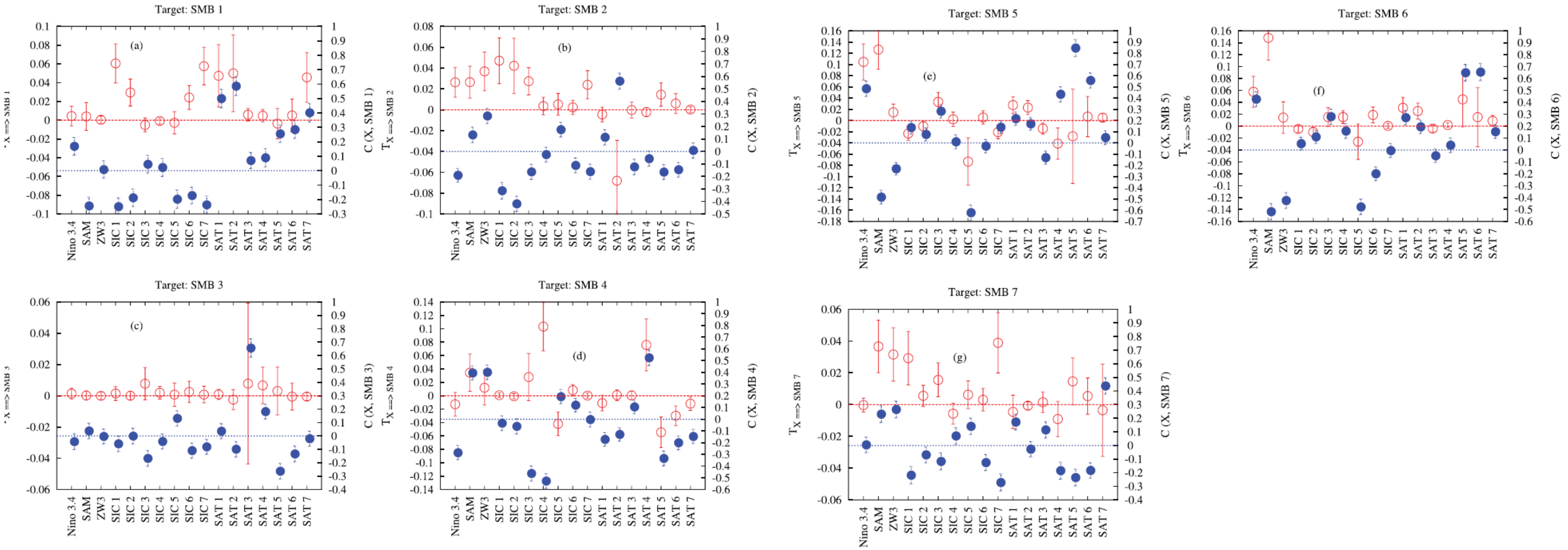

Transfer of information in red and correlation in blue. Target on top of each panel

Results: CESM1-CAM5

Dependence of SMB on Atmospheric Indices:

El-Nino influences Regions 2, 5 and 6

SAM influences Regions 2, 4, 5, 6 and 7

ZW3 influences Regions 2 and 7

Larger set of dependences in this model

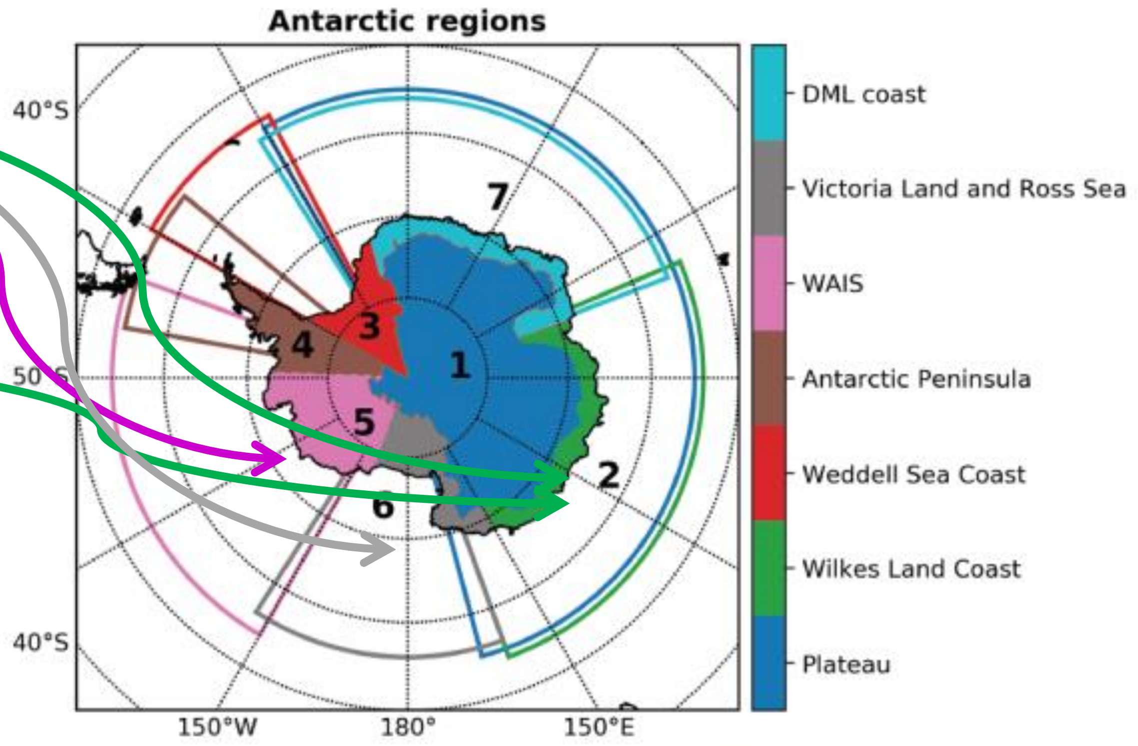

Figure 3. Regional boundaries separating the different regions used in this study. DML = Dronning Maud Land; WAIS = West Antarctica Ice Sheet.

Results: CESM1-CAM5

Dependence of SMB on Surface temperature:

Region 1: influenced by 1, 2, 3 and 7
Region 2: influenced by 2 and 5
Region 4: influenced by 4, 5, 6 and 7
Region 6: influenced by 1, 2 and 7

Dependence of SMB on Sear Ice:

Region 1: influenced by 1, 2, 5, 6 and 7
Region 2: influenced by 1, 2, 3 and 7
Region 4: influenced by 4 and 5
Region 5: influenced by 1, 2, 3, 5 and 7
Region 6: influenced by 4 and 6
Region 7: influenced by 1, 3 and 7

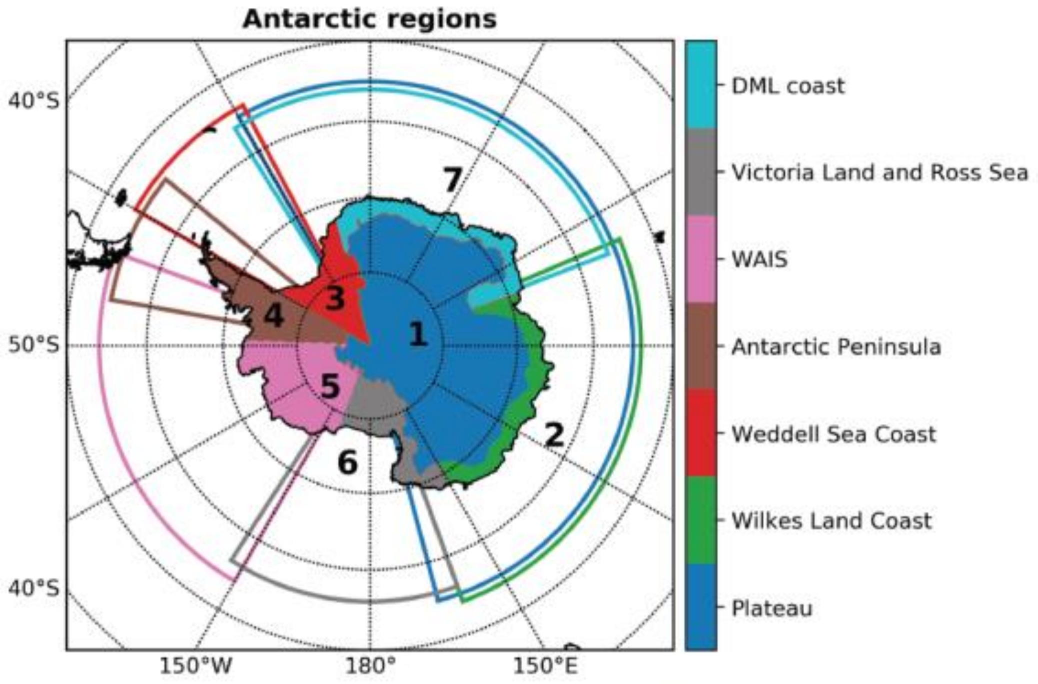

Figure 3. Regional boundaries separating the different regions used in this study. DML = Dronning Maud Land; WAIS = West Antarctica Ice Sheet.

Much stronger influence of SIC on SMB in this model

Key conclusions on dependences

1. Several studies have suggested decreased precipitation over the Antarctic Plateau associated to a positive SAM index (e.g., Marshall et al., 2017; Medley et al., 2018), in agreement with the significant correlation found for both models. Nevertheless, the absence of dependence indicates that the link is not of dynamical nature. Rather, the changes should be associated with local thermodynamic processes in Region 1. If SAM has an influence at all, it would probably be associated with modifications of temperature conditions.

2. Although dynamical connections between SMB and the other observables are stronger in the CESM1-CAM5 model than in MPI-ESM-P, a few key results concerning the dependence of SMB, coherent between the two models, are emerging: (i) The Antarctic Plateau is not influenced by the large-scale modes but well by the SAT and SIC; (ii) the SMB over the Weddell Sea coast and the DML coast are not influenced by the SAT; and (iii) the Weddell Sea coast is not dynamically influenced by the SIC.

Key conclusions (continued)

3. Although the statistics based on correlation are useful to have a first clue on the presence of a link between two observables, it cannot be used to infer any dynamical influence between them. Recent developments on information transfer in dynamical systems provide new tools to investigate dynamical interactions (Liang, 2014). This technique can be easily used for comparing time series.

Reference: Vannitsem, S., Dalaiden, Q., & Goosse, H. (2019). Testing for dynamical dependence: Application to the surface mass balance over Antarctica. *Geophysical Research letters*, *46*, https://doi.org/10.1029/2019GL084329

List of references

Liang, X. S. (2014). Unraveling the cause-effect relation between time series. *Physical Review E*, *90*, 52150.

Liang, X. S., & Kleeman, R. (2005). Information transfer between dynamical system components. *Physical Review E*, *95*, 244101.

Liang, X. S., & Kleeman, R. (2007). A rigourous formalism of information transfer between dynamical system components, II. Continuous flow. *Physica D*, *227*, 173–182.

Marshall, G. J., Thompson, D.W., & van den Broeke, M. R. (2017). The signature of Southern Hemisphere atmospheric circulation patterns in Antarctic precipitation. *Geophysical Research Letters*, *44*, 11,580–11,589. https://doi.org/10.1002/2017GL075998

Medley, B., Mcconnell, J., Neumann, T., Reijmer, C., Chellman, N., Sigl, M., & Kipfstuhl, S. (2018). Temperature and snowfall in western Queen Maud Land increasing faster than climate model projections. *Geophysical Research Letters*, *45*, 1472–1480. https://doi.org/10.1002/2017GL075992

Medley, B., Thomas, E.R. (2019). Increased snowfall over the Antarctic Ice Sheet mitigated twentieth-century sea-level rise. *Nature Clim Change, 9*, 34–39. https://doi.org/10.1038/s41558-018-0356-x

Wang, H., Fyke, J. G., Lenaerts, J. T. M., Nusbaumer, J. M., Singh, H., Noone, D., Rasch, P. J., and Zhang, R. (2020). Influence of sea-ice anomalies on Antarctic precipitation using source attribution in the Community Earth System Model, *The Cryosphere*, *14*, 429–444, https://doi.org/10.5194/tc-14-429-2020, 2020.